

**Title page**

Involvement of the Pyrilamine Transporter, a Putative Organic Cation Transporter, in  
Blood-Brain Barrier Transport of Oxycodone

Takashi Okura, Asami Hattori, Yusuke Takano, Takenori Sato, Margareta  
Hammarlund-Udenaes, Tetsuya Terasaki, and Yoshiharu Deguchi

*Department of Drug Disposition & Pharmacokinetics, School of Pharmaceutical Sciences,  
Teikyo University, Sagamihara, Japan (T.O., A.H., Y.T., T.S., Y.D.)*

*Division of Pharmacokinetics and Drug Therapy, Department of Pharmaceutical Biosciences,  
Uppsala University, Uppsala, Sweden (M.H-U.)*

*Department of Molecular Biopharmacy and Genetics, Graduate School of Pharmaceutical  
Sciences, Tohoku University, Sendai, Japan (T.T.)*

**Running title page**

**a) Running title:** Blood-brain barrier transport of oxycodone

**b) Corresponding author:**

Name: Yoshiharu Deguchi

Organization: Teikyo University

Address: 1091-1 Suarashi, Sagamiko, Sagamihara, Kanagawa 229-0195, Japan

Telephone/FAX: +81-426-85-3766

e-mail address: deguchi@pharm.teikyo-u.ac.jp

**c) Numbers of text pages:** 25

**Numbers of table:** 2

**Numbers of figures:** 8

**Numbers of references:** 31

**Numbers of words in abstract:** 242

**Numbers of words in introduction:** 486

**Numbers of words in discussion:** 1483

**d) Nonstandard abbreviations**

BBB: blood-brain barrier; FCCP: p-trifluoromethoxyphenyl-hydrazone; MATE: multidrug and toxin extrusion; MPP<sup>+</sup>: 1-methyl-4-phenylpyridinium; OCT: organic cation transporter; pHi: intracellular pH; TEA: tetraethylammonium; TR-BBB13: conditionally immortalized rat brain capillary endothelial cells

## Abstract

The purpose of this study is to characterize blood-brain barrier (BBB) transport of oxycodone, a cationic opioid agonist, via the pyrilamine transporter, a putative organic cation transporter, using conditionally immortalized rat brain capillary endothelial cells (TR-BBB13). Oxycodone and [ $^3\text{H}$ ]pyrilamine were both transported into TR-BBB13 cells in a temperature- and concentration-dependent manner with  $K_m$  values of 89  $\mu\text{M}$  and 28  $\mu\text{M}$ , respectively. The initial uptake of oxycodone was significantly enhanced by preloading with pyrilamine, and vice versa. Further, mutual uptake inhibition by oxycodone and pyrilamine suggests that a common mechanism is involved in their transport. Transport of both substrates was inhibited by type II cations (quinidine, verapamil, amantadine), but not by classic OCT substrates and/or inhibitors (TEA, MPP, corticosterone), substrates of OCTN1 (ergothioneine) and OCTN2 (L-carnitine), or organic anions. The transport was inhibited by metabolic inhibitors (rotenone, sodium azide), but was insensitive to extracellular sodium and membrane potential for both substrates. Further, the transport of both substrates was increased at alkaline extracellular pH, and decreased in the presence of a protonophore (FCCP). Intracellular acidification induced with ammonium chloride enhanced the uptakes, suggesting that the transport is driven by an oppositely directed proton gradient. The brain uptake of oxycodone measured by in situ rat brain perfusion was increased in alkaline perfusate and was significantly inhibited by pyrilamine. These results suggest that BBB transport of oxycodone is at least partly mediated by a common transporter with pyrilamine, and this transporter is an energy-dependent, proton-coupled antiporter.

## Introduction

The blood-brain barrier (BBB) is formed by the brain capillary endothelium and regulates the paracellular permeability of both large and small hydrophilic molecules (Pardridge, 2005). It is well known that the supply of nutrients from the circulating blood into the brain across the BBB is controlled by a number of transporters, such as sodium-independent glucose transporter (GLUT1, *SLC2A1*), monocarboxylate transporter (MCT1, *SLC16A1*), and large neutral amino acid transporter (LAT1, *SLC7A5*) with 4F2hc (*SLC3A2*). Not only nutrients, but also several drugs are translocated into the brain across the BBB. For example, MCT1 and LAT1 transport L-dopa (Kageyama et al., 2000; Gomrs & Soares-da-Silva, 1999). Organic anion transporter 3 (OAT3, *SLC22A8*) and/or organic anion transport polypeptide (Oatp1a4, *Slco1a4*) mediate the efflux transport of endogenous metabolites (Mori et al., 2003) and several anionic drugs, such as digoxin (Kusuhara et al., 1999), simvastatin (Tsuji, 2005) and 6-mercaptopurine (Mori et al., 2004; Deguchi et al., 2000) across the BBB.

In relation to the membrane transport of cationic drugs, at least 6 distinct transporters OCT1 (*SLC22A1*), OCT2 (*SLC22A2*), OCT3 (*SLC22A3*), OCTN1 (*SLC22A4*), OCTN2 (*SLC22A5*), MATE1 (*SLC47A1*)) for organic cations are involved in the influx and efflux transport of various cations in the kidney and liver (Nezu et al., 1999; Inui et al., 2000; Koepsell, 2003; Otsuka et al., 2005). However, relatively little is known what transporters are involved in the BBB transport of cationic drugs. Yamazaki et al. (1994a,b,c) demonstrated that pyrilamine, a cationic H<sub>1</sub>-antagonist, is transferred from the circulating blood into the brain by an organic cation-sensitive transport system. Recently, we reported that pramipexole, a potent dopamine receptor agonist with high efficacy for Parkinson's disease, is also transported across the BBB via the organic cation-sensitive transporter (Okura, 2007). Therefore, the putative pyrilamine transporter has been suggested to be an organic cation transporter at the BBB, although its molecular species remains to be

identified.

Oxycodone is widely used as an opioid agonist for treatment of moderate to severe cancer pain. Boström et al. (2006) have recently reported that the steady-state unbound concentration of oxycodone in the brain interstitial fluid is 3-fold higher than that in the plasma, suggesting the existence of an active influx transporter(s) for oxycodone at the BBB. Oxycodone is a weak cationic drug with a partial positive charge at physiological pH, so the pyrilamine transporter may mediate the transport of oxycodone across the BBB.

The purpose of this study, therefore, is to clarify the BBB transport properties of oxycodone across the BBB and the role of the pyrilamine transporter. The transports of oxycodone and pyrilamine were characterized using conditionally immortalized rat brain capillary endothelial cells (TR-BBB13) as an *in vitro* model of the BBB. Further, *in vivo* BBB transport of oxycodone was examined by the *in situ* rat brain perfusion technique. The results obtained in this study should provide useful information for the development and proper use of CNS-acting cationic drugs, as well as for pain therapy with opioids.

## Materials and Methods

**Chemicals.** Oxycodone was kindly provided by Takeda Pharmaceutical Co. Ltd. (Osaka, Japan). [ $^3\text{H}$ ]Pyrilamine (23 – 30 Ci/mmol) and [ $^3\text{H}$ ]inulin (0.59 Ci/mmol) were purchased from Amersham Bioscience (Buckinghamshire, UK). All other chemicals and reagents were commercial products of reagent grade.

**Animals.** Adult male Wistar rats weighing about 350 g were purchased from Japan SLC (Shizuoka, Japan); they were housed, three or four per cage, in a laboratory with free access to food and water and were maintained on a 12-hr dark/12-hr light cycle in a room with controlled temperature ( $24 \pm 2^\circ\text{C}$ ) and humidity ( $55 \pm 5\%$ ). This study was conducted according to guidelines approved by the Experimental Animal Ethical Committee of Teikyo University.

**Transport studies in TR-BBB13 cells.** TR-BBB13 cells were seeded on collagen-coated multiwell dishes at a density of  $0.1 \times 10^5$  cells/cm $^2$ . At 3 days after seeding, the cells were washed twice with 1 mL of PBS and preincubated with incubation buffer (122 mM NaCl, 3 mM KCl, 25 mM NaHCO $_3$ , 1.2 mM MgSO $_4$ , 1.4 mM CaCl $_2$ , 10 mM D-glucose, 10 mM HEPES, pH 7.4) for 20 min at  $37^\circ\text{C}$ . After preincubation, the buffer (0.25 mL) containing oxycodone (30  $\mu\text{M}$ ) or [ $^3\text{H}$ ]pyrilamine (74 kBq/ $\mu\text{L}$ , 90 nM) was added to initiate uptake. The cells were incubated at  $37^\circ\text{C}$  for a designated time, and then washed three times with 1 mL of ice-cold incubation buffer to terminate the uptake. The cells were collected and homogenized by sonication in 300  $\mu\text{L}$  of water, and the homogenate was stored at  $-20^\circ\text{C}$  until determination of oxycodone as described below. For the determination of [ $^3\text{H}$ ]pyrilamine radioactivity, the cells were solubilized with 1 N NaOH for 60 min. The radioactivity was measured using a liquid scintillation counter after the addition of scintillation cocktail Hionic Fluor (PerkinElmer Life and Analytical Sciences). Cellular protein content was determined with a BCA protein assay kit (Pierce Chemical Co., Rochford, IL, USA). Uptake was expressed as

DMD# 22087

the cell-to-medium ratio ( $\mu\text{L}/\text{mg}$  protein) obtained by dividing the uptake amount by the concentration of substrate in the incubation buffer. In order to estimate the kinetic parameters for the uptake by TR-BBB13 cells, the initial uptake rates for oxycodone ( $1 - 500 \mu\text{M}$ , for 15 sec) and [ $^3\text{H}$ ]pyrilamine ( $6 - 500 \mu\text{M}$ , for 10 sec) were determined by subtracting the uptakes at the concentration of 5 mM oxycodone and pyrilamine, respectively. The initial uptake rates were fitted to the following equation by means of nonlinear least-squares regression analysis with Prism software (Graphpad, San Diego, CA, USA):

$$v = \frac{V_{\max} \times s}{K_m + s}$$

where  $v$  is the initial uptake rate of substrate (nmol/min/mg protein),  $s$  is the substrate concentration in the medium ( $\mu\text{M}$ ),  $K_m$  is the Michaelis-Menten constant ( $\mu\text{M}$ ) and  $V_{\max}$  is the maximum uptake rate (nmol/min/mg protein). In Lineweaver-Burk plot analysis, the initial uptake rate was In the trans-stimulation studies, the cells were preloaded with pyrilamine ( $250 \mu\text{M}$ ) or oxycodone ( $1 \text{ mM}$ ) for 20 min. Cells were then rinsed with 1 mL of incubation medium warmed at  $37^\circ\text{C}$ . Subsequently, uptake of oxycodone or [ $^3\text{H}$ ]pyrilamine by the cells was measured. In the inhibition study, the uptake was measured after incubation with oxycodone ( $30 \mu\text{M}$ ) for 15 sec or [ $^3\text{H}$ ]pyrilamine ( $74 \text{ kBq}/\mu\text{L}$ ,  $90 \text{ nM}$ ) for 10 sec, respectively, in the presence of several inhibitors. After treatment with  $25 \mu\text{M}$  rotenone or  $0.1\%$   $\text{NaN}_3$  for 20 min to reduce metabolic energy, the uptakes of oxycodone and [ $^3\text{H}$ ]pyrilamine were measured as described above. Uptake was also measured at medium pH values of 7.4 and 8.4 in the presence or absence of  $10 \mu\text{M}$  p-trifluoromethoxyphenyl-hydrazone (FCCP) a protonophore. When the influence of intracellular pH (pHi) was examined, the uptake was measured in the presence of  $30 \text{ mM}$   $\text{NH}_4\text{Cl}$  to elevate pHi (Terada et al., 2006; Ohta et al., 2006). To measure the uptake at acidic pHi, extracellular  $\text{NH}_4\text{Cl}$  was removed after the

DMD# 22087

preincubation with 30 mM NH<sub>4</sub>Cl, because intracellular NH<sub>3</sub> rapidly diffuses out of the cells, resulting in the accumulation of protons released from NH<sub>4</sub><sup>+</sup> during NH<sub>3</sub> generation in the cells.

**In situ brain perfusion study.** Brain perfusion was performed by the method reported previously (Takasato et al., 1984). In brief, each rat was anesthetized and the right carotid artery was catheterized with polyethylene tubing (SP-10) filled with sodium heparin (100 IU/mL). The perfusate (Krebs-Henseleit buffer, 118 mM NaCl, 4.7 mM KCl, 25 mM NaHCO<sub>3</sub>, 1.2 mM KH<sub>2</sub>PO<sub>4</sub>, 2.5 mM CaCl<sub>2</sub>, 1.2 mM MgSO<sub>4</sub>, 10 mM D-glucose, pH 7.4) containing oxycodone (30 μM) and [<sup>3</sup>H]inulin (0.9 μM), a brain intravascular marker, was passed through the catheter at the rate of 4.9 mL/min with an infusion pump (Harvard Apparatus, South Natick, MA, USA). After the infusion pump is started, 5.0 sec is required to fill the external carotid artery cannula (Takasato et al., 1984). Therefore 5.0 sec was subtracted routinely from the gross perfusion time in each experiment, to obtain uptake time for which perfusate was actually within the brain capillary. At the end of uptake for 0 – 30 sec, rats were decapitated, and the right cerebral hemisphere was dissected from the perfused brain and weighed. The brain samples were stored at –20°C until determination of oxycodone. The value of the permeability-surface area product (PS<sub>BBB,inf</sub>), which represents in vivo BBB permeability, was calculated from the following equation after correcting for remaining intravascular oxycodone, estimated from the apparent brain uptake of [<sup>3</sup>H]inulin:

$$PS_{BBB,inf} \text{ value } (\mu\text{L}/\text{min}/\text{g brain}) = -F_{pf} \times \ln(1 - K_{in} / F_{pf})$$

where F<sub>pf</sub> is the flow rate of the perfusate (7.54 mL/min/g brain) (Takasato et al., 1984), and K<sub>in</sub> is a transfer constant. The flow rate substantially exceeded the K<sub>in</sub> value, indicating that the flow rate is not the limiting factor for the brain transport of oxycodone. The transfer



constant ( $K_{in}$ ) for unidirectional uptake was calculated by fitting the equation:

$$q_{br} / C_{pf} = K_{in} \times T + V_0$$

where  $q_{br}$  is the amount of oxycodone in the brain,  $C_{pf}$  is the concentration of oxycodone in the perfusate,  $T$  is uptake time (min) and  $V_0$  is the extrapolated oxycodone intercept ( $T = 0$ ).

**Determination of oxycodone.** Oxycodone was determined by HPLC with electrochemical detection (ECD) (Kokubun et al., 2005). Twenty  $\mu$ L of codeine solution (250 ng/mL), an internal standard, 100  $\mu$ L of 4 N NaOH and 800  $\mu$ L of butyl chloride were added to 200  $\mu$ L of cell homogenate. The samples were mixed, and centrifuged for 10 min at 3000 rpm at 4°C, then the butyl chloride layer was transferred. The remaining aqueous layer was extracted again with 800  $\mu$ L of butyl chloride. The combined butyl chloride extract was evaporated to dryness. The residue was reconstituted in 200  $\mu$ L of mobile phase, and a 40  $\mu$ L aliquot was injected into the HPLC. The cerebral hemisphere was homogenized in 5 volumes of perchloric acid, and the homogenate was centrifuged for 10 min at 3000 rpm at 4°C. Naltrexone solution (250 ng/mL) was added as an internal standard to the supernatant, and the solution was neutralized and subjected to solid-phase extraction using an Oasis HLB cartridge (Waters, Milford, MA, USA). The Oasis HLB cartridge was first pre-wetted with methanol (1 mL), followed by water (1 mL). The sample was applied to the cartridge, the cartridge was washed with 1 mL of 5% methanol, and oxycodone and naltrexone were then eluted with methanol. The eluate was dried under a nitrogen stream and the residues were reconstituted in the HPLC mobile phase. The HPLC system consisted of a pump (301E, Eicom, Kyoto, Japan), an electrochemical detector (ECD-300, Eicom, Kyoto, Japan). The HPLC analytical column used was an XTerra® RP18 (4.6 mm x 50 mm, 5  $\mu$ m particle size, Waters). The HPLC separation for oxycodone, codeine and naltrexone was carried out at a flow rate of 0.5

DMD# 22087

mL/min with a mobile phase containing 10% acetonitrile, 20% methanol and 5 mM phosphate buffer (pH 8.0) at 40°C. The retention times of oxycodone, codeine and naltrexone were 9.1, 6.4 and 23.3 min, respectively. The voltage of the working electrode of the electrochemical detector was set at 800 mV. Standard curves of oxycodone in the amount range of 0.15 – 50 pmol injected onto the column showed good linearity (coefficient of determination > 0.99). The detection limit for quantification of oxycodone was 3 nM. Runs were accepted if the precision and accuracy of the quality control samples at low (3 nM), middle (10 nM) and high (100 nM) concentrations had a coefficient of variation (CV) below 15%.

**Expression profiling of organic cation transporters by real-time PCR.** The mRNA levels of organic cation transporters (rOCT1-3, rOCTN1-2, rMATE1) in TR-BBB13 cells were measured by quantitative real-time PCR analysis. Total RNA was isolated from TR-BBB13 cells and rat brain and kidney using an RNeasy mini kit (Qiagen, Valencia, CA, USA). Single-strand cDNA was prepared from 1.0 µg of total RNA by RT (Superscript III, Invitrogen, Carlsbad, CA, USA) using oligo (dT) primer. Quantitative real-time PCR analysis was performed using a 7500 sequence detection system (PE Applied Biosystems, Foster City, CA, USA) with 2x SYBR Green PCR Master Mix (PE Applied Biosystems ) according to the manufacturer's protocols. Rat genomic DNA was used as a standard in quantitative PCR. The sense and antisense primers were 5'-TTC ACC CCT GGA CAT TAT TGC-3' and 5'-TCA TGC ACT GGC TGA GGA AG-3' for rOCT1, 5'-CCC CAA ACC CAC ACA AAC C-3' and 5'-CAA CAG ACC GTG CAA GCT ACA-3' for rOCT2, 5'-CCC TGT GTG TTT CAT GGC TGT-3' and 5'-CTT GAA ATG CAA TCC AAA GGC-3' for rOCT3, 5'-GGG ACA GGA GGA TCG AGA AGT-3' and 5'-GGC TGG TCT CAC ACT CCT GAC-3' for rOCTN1, 5'-CGC AAA AAG ATG GTG GAG AAA-3' and 5'-CAG GGT GTT AGA AGG CTG TGC-3' for rOCTN2, 5'- TGC CAT CGG CTA TTA TGT CAT C-3' and 5'- AGC TTG GCA ACG AAC ATC AGT-3' for rMATE1 and 5'-GGT GGA CCT CAT GGC CTA

DMD# 22087

CAT-3' and 5'-TGG GTG GTC CAG GGT TTC T-3' for rGAPDH. All primers were designed on the basis of the published full sequence of each transporter. The thermal protocol was set to 2 min at 50°C, followed by 10 min at 95°C, and then 40 cycles of 15 s at 95°C and 1 min at 60°C. To confirm specificity of amplification, the PCR products were subjected to a melting curve analysis. The control lacking the RT enzyme was assayed in parallel to monitor any possible genomic contamination.

**Statistical analysis.** Statistical analysis of the data was performed by employing Student's t-test and by one-way analysis of variance followed by Dunnett's test for single and multiple comparisons, respectively. Differences were considered statistically significant at  $P < 0.05$ .

## Results

**Uptake kinetics of oxycodone and [ $^3\text{H}$ ]pyrilamine by TR-BBB13 cells.** The uptake of oxycodone increased with time at 37°C, and the cell-to-medium ratio was 40.5 – 40.9 at 30 – 60 sec (Fig 1A). The uptake at 4°C was decreased by 41 – 68% compared with that at 37°C. [ $^3\text{H}$ ]Pyrilamine uptake by TR-BBB13 cells also increased with time, and the cell-to-medium ratio was 68.5 at 60 sec. The uptake was decreased by 53 – 62 % at 4°C (Fig. 1B). The initial uptake was assessed as the uptake at 15 sec for oxycodone and 10 sec for [ $^3\text{H}$ ]pyrilamine, respectively, in the subsequent kinetic and inhibition studies. The initial uptakes of oxycodone and [ $^3\text{H}$ ]pyrilamine were concentration-dependent (Fig. 2). Each Eadie-Hofstee plot gave a single straight line, indicating a single saturable process. Kinetic analysis provide a  $K_m$  value of 89  $\mu\text{M}$  and a  $V_{\max}$  of 3.5 nmol/mg protein/15 sec for oxycodone, and a  $K_m$  value of 28  $\mu\text{M}$  and a  $V_{\max}$  of 0.7 nmol/mg protein/10 sec for [ $^3\text{H}$ ]pyrilamine.

**Trans-stimulation study on the uptakes of oxycodone and [ $^3\text{H}$ ]pyrilamine by TR-BBB13 cells.** To examine whether the initial uptake of oxycodone might be attributable to membrane transport or binding to the membrane surface and intracellular components, a trans-stimulation study on the initial uptake of oxycodone into TR-BBB13 cells was carried out (Fig. 3). The oxycodone uptake was significantly enhanced by preloading with 250  $\mu\text{M}$  pyrilamine for 20 min. [ $^3\text{H}$ ]Pyrilamine uptake was also increased by pretreatment with 1 mM oxycodone.

**Inhibition study on the uptakes of oxycodone and [ $^3\text{H}$ ]pyrilamine by TR-BBB13 cells.** In Lineweaver-Burk plot analyses of mutual inhibitory effects on uptake of oxycodone and pyrilamine (Fig. 4), the plots of oxycodone uptake in the presence and absence of pyrilamine intersected at the ordinate axis. This result indicated that pyrilamine competitively inhibited oxycodone uptake with a  $K_i$  value of 30  $\mu\text{M}$ . Oxycodone also competitively inhibited pyrilamine uptake with a  $K_i$  value of 135  $\mu\text{M}$ . These mutual and competitive inhibitions

between oxycodone and pyrilamine suggest that a common transporter(s) is involved in their influx transport into the TR-BBB13 cells, at least in part. In the inhibition study, the uptakes of oxycodone and [ $^3\text{H}$ ]pyrilamine were inhibited by cationic compounds such as quinidine, verapamil, amantadine, serotonin, but not TEA, MPP, or corticosterone (classic substrates and/or inhibitors of OCTs) (Table 1). Choline and hemicholinium-3 (substrates or inhibitors of the choline transport system) had no or only a slight inhibitory effect on these uptakes. Ergothioneine (an OCTN1-specific substrate), L-carnitine (an OCTN2-specific substrate), p-aminohippuric acid (a substrate of OAT3) and digoxin (a substrate of OATP) did not affect these uptakes.

**Metabolic energy and ion dependence of the uptakes of oxycodone and [ $^3\text{H}$ ]pyrilamine by TR-BBB13 cells.** The uptakes of oxycodone and [ $^3\text{H}$ ]pyrilamine were significantly inhibited by pretreatment with rotenone and sodium azide in TR-BBB13 cells (Fig. 5). The uptakes of oxycodone and [ $^3\text{H}$ ]pyrilamine were not affected by the replacement of extracellular  $\text{Na}^+$  with *N*-methylglucamine $^+$  (Fig. 6). Treatment with valinomycin, a potassium ionophore, did not significantly change the uptake of these drugs. The pH dependence of the uptake is shown in Fig. 7. The uptakes of oxycodone and [ $^3\text{H}$ ]pyrilamine were increased at higher extracellular pH (8.4), and decreased by treatment with FCCP, a protonophore (Fig. 7A and B). To examine the effect of the intracellular pH, the cells were treated with  $\text{NH}_4\text{Cl}$ , because intracellular pH rises in the presence of  $\text{NH}_4\text{Cl}$  (acute treatment), and subsequent removal of  $\text{NH}_4\text{Cl}$  (pretreatment) causes a decrease in intracellular pH (Terada et al., 2006; Ohta et al., 2006). Acute treatment with  $\text{NH}_4\text{Cl}$  (intracellular alkalization) markedly reduced the uptakes of oxycodone (Fig. 7C) and [ $^3\text{H}$ ]pyrilamine (Fig. 7D), while pretreatment with  $\text{NH}_4\text{Cl}$  (intracellular acidification) resulted in stimulation of oxycodone uptake, but not [ $^3\text{H}$ ]pyrilamine uptake, at extracellular pH 8.4.

***In vivo* blood-to-brain transport of oxycodone.** The brain uptake of oxycodone was

DMD# 22087

measured by the in situ brain perfusion technique. The brain/perfusate (B/P) ratio of oxycodone linearly increased with increasing perfusion time up to 30 sec (Fig. 8A). The  $PS_{BBB,inf}$  value for oxycodone was 224  $\mu\text{L}/\text{min}/\text{g}$  brain, which is 20 times greater than the value for brain uptake clearance of morphine (11.4  $\mu\text{L}/\text{min}/\text{g}$  brain) (Tunblad et al., 2003) and one-seventh of the value for [ $^3\text{H}$ ]pyrilamine (1618  $\mu\text{L}/\text{min}/\text{g}$  brain) (Yamazaki et al., 1994). The B/P ratio at time 0 sec was  $0.044 \pm 0.008$  mL/g brain. This value was 4-fold greater than the measured vascular [ $^3\text{H}$ ]inulin space of  $0.011 \pm 0.001$  mL/g brain. This value of vascular [ $^3\text{H}$ ]inulin space is consistent with reported values (0.007 – 0.017 mL/g brain) (Takasato et al., 1984; Allen & Smith, 2001). This suggests that B/P ratio at time 0 sec may include a contribution due to extremely rapid binding to the capillary surface. The observation of this rapidly equilibrating component of brain oxycodone uptake emphasizes the importance of a thorough time-course analysis to estimate the BBB permeability of cationic compounds, taking account of simple binding or association with the luminal membrane of the brain capillary endothelium (Allen & Smith, 2001). The brain uptake at pH 7.4 for 15-sec perfusion, corrected for the rapidly equilibrating component of oxycodone, was significantly inhibited by 54 % by co-perfusion with 1 mM pyrilamine (Fig. 8B). The brain uptake of oxycodone was increased by 4.4-fold in alkaline perfusate (pH 8.4), compared with that at pH 7.4. The brain uptake at pH 8.4 was also decreased by 45% by co-perfusion of 1 mM pyrilamine.

**mRNA expression of organic cation transporters in TR-BBB13 and rat brain capillary.** To provide molecular evidence for the expression of organic cation transporters in TR-BBB13 cells, the mRNA expression levels of rOCT1, rOCT2, rOCT3, rOCTN1, rOCTN2, rMATE1 and rGAPDH in TR-BBB13 cells were determined by quantitative RT-PCR analysis (Table 2). A relatively high mRNA expression of rOCTN2 was found in TR-BBB13 cells. The rOCTN2 mRNA expression in TR-BBB13 cells was greater than that in the brain. On the other hand, the expression levels of rOCT1-3, rOCTN1 and rMATE1 were negligible or low

DMD# 22087

in TR-BBB13 cells.

## Discussion

The BBB transport of CNS-acting drugs is an important determinant of their pharmacological action in the CNS. Here, the role of the pyrilamine transporter, a putative cation transporter, in the BBB transport of oxycodone, a cationic opioid, was characterized, using TR-BBB13 cells. The results indicate that transport of both oxycodone and pyrilamine is mediated by an energy-dependent, proton-coupled antiporter. Further, *in situ* brain perfusion indicated that the pyrilamine transporter is involved in oxycodone transport into the brain across the BBB.

TR-BBB13 cells are stable, immortalized rat brain capillary endothelial cells derived from transgenic rats harboring temperature-sensitive SV40 large-T antigen (Terasaki et al., 2003). They express several transporters, including GLUT1, MCT1, LAT1 with 4F2hc (Hosoya et al., 2000) and OAT3 (Ohtsuki et al., 2002), and these transporters are functional. TR-BBB13 cells retain glucose transport function with 10-fold higher activity than that of primary-cultured bovine brain endothelial cells (Terasaki et al., 2003). Further, the BBB permeability clearances of several compounds estimated in TR-BBB13 cells were quite similar to those measured *in vivo* (Terasaki et al., 2003). Therefore, this cell line appears to be suitable as an *in vitro* BBB model for investigating BBB transport mechanisms.

The uptakes of oxycodone and [ $^3\text{H}$ ]pyrilamine were time- and temperature-dependent. The values of the cell-to-medium ratio for oxycodone and [ $^3\text{H}$ ]pyrilamine reached 40 and 70, respectively, at 60 sec, suggesting that both cationic drugs are concentrated into the cells and/or bound to the intracellular constituents of TR-BBB13 cells after having passed through the cell membrane. The uptakes of oxycodone and [ $^3\text{H}$ ]pyrilamine by TR-BBB13 cells were saturable (Fig. 2). Saturation of uptake could be explained by not only saturation of the membrane transport, but also by saturation of membrane surface binding and/or intracellular binding. Therefore, trans-stimulation studies were carried out to confirm that the initial uptake



obtained here is attributable to transport through the plasma membrane. The initial uptake of oxycodone was significantly enhanced by preloading with pyrilamine and vice versa (Fig. 3). These results suggest that saturation of oxycodone and pyrilamine uptake is caused by the saturation of a specific transport system at the membrane of TR-BBB13 cells. In addition, kinetic analyses revealed that the calculated uptake clearance ( $V_{max}/K_m$ ) for oxycodone (157  $\mu\text{L}/\text{min}/\text{mg}$  protein) was in good agreement with that of [ $^3\text{H}$ ]pyrilamine (150  $\mu\text{L}/\text{min}/\text{mg}$  protein), suggesting participation of a transport system with similar affinity and transport rate for the two substrates. The  $K_m$  values for the serotonin transporter (SERT) and the norepinephrine transporter (NET) are 0.1 – 0.5  $\mu\text{M}$ . Therefore, oxycodone transport in TR-BBB13 cells may be mediated by a relatively low-affinity transporter different from the  $\text{Na}^+$ -dependent transporters for endogenous cationic neurotransmitters.

To examine commonality in the transport of oxycodone and pyrilamine, mutual inhibitory kinetic studies were carried out. Oxycodone and pyrilamine indeed mutually inhibited the uptake of each other (Fig. 4). The  $K_i$  values estimated for oxycodone (135  $\mu\text{M}$ ) and for pyrilamine (30  $\mu\text{M}$ ) were similar to respective  $K_m$  values for oxycodone (89  $\mu\text{M}$ ) and pyrilamine (28  $\mu\text{M}$ ), suggesting the occurrence of competition between oxycodone and pyrilamine for binding to the transporter.

Bulky hydrophobic cations with widely differing molecular structures, such as pyrilamine, quinidine, verapamil and amantadine, markedly inhibited the transports of oxycodone and [ $^3\text{H}$ ]pyrilamine into TR-BBB13 cells (Table 1). These data suggest that the putative pyrilamine transporter may be polyspecific. In contrast, organic cations which are classic substrates of OCTs, such as TEA and MPP, had no significant effect. This finding suggests that oxycodone and pyrilamine transports are mediated by an organic cation-sensitive transporter, but the interaction does not involve electrostatic interaction as in the case of cationic peptides (Deguchi et al., 2003). Ergothioneine (a specific substrate of OCTN1),

DMD# 22087

L-carnitine (an endogenous substrate of OCTN2), choline and hemicholinium-3 (representative substrate and inhibitor, respectively, of the choline transport system), or organic anions showed no or only slight inhibition, suggesting that rOCTN1, rOCTN2, choline transporter and organic anion transporter may not play major roles in oxycodone and pyrilamine transport.

To identify the driving force for oxycodone and pyrilamine transport, the effects of metabolic inhibitors and extracellular ions were examined. The transports of both drugs were significantly inhibited by pretreatment with metabolic inhibitors, but were insensitive to extracellular sodium and membrane potential in TR-BBB13 cells. The uptakes of oxycodone and [ $^3\text{H}$ ]pyrilamine were increased at higher extracellular pH (8.4), and decreased in the presence of FCCP. Intracellular acidification induced with  $\text{NH}_4\text{Cl}$  resulted in stimulation of the uptakes. These results suggest that the transport is dependent on an oppositely-directed proton gradient. The intracellular pH in rat brain capillary endothelial cells has been estimated to be 6.9 – 7.15 (Sipos et al., 2005; Taylor et al., 2006). Lower intracellular pH than extracellular pH can drive organic cation/ $\text{H}^+$  antiport. Thus, an energy- and proton-dependent transporter seems to be involved in oxycodone and pyrilamine uptakes in TR-BBB13 cells. This organic cation/ $\text{H}^+$  antiporter at the BBB could play a role in establishing the sustained unbound concentration gradient of oxycodone between the brain interstitial fluid and the blood, observed by in vivo microdialysis in rats (Boström et al., 2006).

[ $^3\text{H}$ ]Pyrilamine transport in primary-cultured bovine brain capillary endothelial cells has been reported to be insensitive to metabolic inhibitors (Yamazaki et al., 1994a). The difference in metabolic energy dependency between primary and immortalized cells may be explained partially by taking differences in expression of transporters into account, because ATP-dependent efflux transporters such as P-glycoprotein and MRP4 are down-regulated in TR-BBB13 cells. Therefore, the net uptake of [ $^3\text{H}$ ]pyrilamine in primary-cultured bovine

brain capillary endothelial cells may be offset by decreases in the efflux rate by metabolic inhibitors.

The in situ brain perfusion technique was employed in order to examine whether the pyrilamine transporter plays a significant role in the BBB transport of oxycodone in vivo. The influx BBB permeability per capillary surface area is estimated to be  $2.24 \mu\text{L}/\text{min}/\text{cm}^2$ , assuming that the rat brain capillary surface area is  $100 \text{ cm}^2/\text{g}$  of brain (Terasaki et al., 2003). This value approximates to the uptake clearance ( $7.14 \mu\text{L}/\text{min}/\text{cm}^2$ ) extrapolated from the in vitro uptake study, despite the down-regulation of P-glycoprotein level in TR-BBB13 cells, indicating that the contribution of the efflux transporter to the brain uptake of oxycodone is not large. Indeed, Boström et al. (2006) reported that the pharmacokinetics of oxycodone in rats was unaffected by co-administration of PSC833, an inhibitor of several efflux transporters including P-glycoprotein and breast cancer resistance protein. The influx BBB permeability of oxycodone in this study was 20 times greater than the reported value for morphine (Tunblad et al., 2003). The difference in the influx BBB permeability between oxycodone and morphine may be partially explained by the P-glycoprotein-mediated active efflux of morphine. However, this does not account for the efficient influx BBB permeability of oxycodone, because the steady-state unbound concentration of oxycodone in the brain interstitial fluid is 3-fold higher than that in the plasma (Boström et al., 2006). An alternative explanation is participation of an active influx transporter(s) for oxycodone at the BBB. The brain uptake of oxycodone was increased in alkaline perfusate (pH 8.4), and it was significantly inhibited by 54% at pH 7.4 and by 45% at pH 8.4 by pyrilamine. The inhibition by pyrilamine is thought to be specific to oxycodone transport, because the co-perfusion with pyrilamine did not change the brain uptake of antipyrine, a BBB transfer marker (unpublished data). These results strongly suggest that the pH- and pyrilamine-sensitive transporter contributes substantially to the efficient transport of oxycodone into the brain across the BBB.

DMD# 22087

This influx transport system at the BBB may play an important role in determining the onset of the analgesic effect and clinical therapeutic outcome of oxycodone.

Quantitative RT-PCR analysis showed that the expression level of rOCTN2 was the highest among the organic cation transporters examined. On the other hand, little or no expression of rOCT1-3 and rMATE1 was observed. Expression levels of these mRNAs in TR-BBB13 cells were similar to those reported in rat brain capillary endothelial cells (RBEC1) (Okura et al., 2007). Lack of mRNA expression of these transporters suggests that OCTs and MATE1 do not play major roles in the transport of cationic drugs in this in vitro BBB model. rOCTN2 has been reported to be involved in L-carnitine transport across the BBB (Kido et al., 2001). The lack of any inhibitory effect of L-carnitine on transports of oxycodone and [<sup>3</sup>H]pyrilamine suggests that rOCTN2 is not the putative pyrilamine transporter. An unidentified organic cation transport system different from previously identified organic cation transporters (OCTs, OCTNs and MATE1) seems to be a candidate for the pyrilamine transporter.

In conclusion, our results indicate that oxycodone is transported into TR-BBB13 cells by the pyrilamine transporter, previously proposed as a putative cation transporter. The transporter was energy-dependent and oppositely directed proton gradient-dependent, but sodium- or membrane potential-independent. It was found that the pyrilamine transporter is also involved in the transport of oxycodone into the brain across the BBB in vivo, though the transport molecule remains unidentified. These findings should be relevant to the treatment of cancer pain with oxycodone, and more generally, to the BBB transport of CNS-acting cationic drugs.

DMD# 22087

## **Acknowledgments**

We gratefully acknowledge the technical support of Drs. Hikaru Yabuuchi and Masaaki Takemura (GenoMembrane Inc.).

## References

- Allen DD and Smith QR (2001) Characterization of the blood-brain barrier choline transporter using the in situ rat brain perfusion technique. *J Neurochem* **76**:1032-41.
- Boström E, Simonsson US and Hammarlund-Udenaes M (2005) Oxycodone pharmacokinetics and pharmacodynamics in the rat in the presence of the P-glycoprotein inhibitor PSC833. *J Pharm Sci* **94**:1060-1066.
- Boström E, Simonsson US and Hammarlund-Udenaes M (2006) In vivo blood-brain barrier transport of oxycodone in the rat: indications for active influx and implications for pharmacokinetics/pharmacodynamics. *Drug Metab Dispos* **34**:1624-1631.
- Deguchi Y, Yokoyama Y, Sakamoto T, Hayashi H, Naito T, Yamada S and Kimura R (2000) Brain distribution of 6-mercaptopurine is regulated by the efflux transport system in the blood-brain barrier. *Life Sci* **66**:649-662.
- Deguchi Y, Miyakawa Y, Sakurada S, Naito Y, Morimoto K, Ohtsuki S, Hosoya K and Terasaki T (2003) Blood-brain barrier transport of a novel  $\mu_1$ -specific opioid peptide, H-Tyr-D-Arg-Phe-beta-Ala-OH (TAPA). *J Neurochem* **84**:1154-1161.
- Gomes P and Soares-da-Silva P (1999) Interaction between L-DOPA and 3-O-methyl-L-DOPA for transport in immortalised rat capillary cerebral endothelial cells. *Neuropharmacology* **38**:1371-1380.
- Hosoya K, Takashima T, Tetsuka K, Nagura T, Ohtsuki S, Takanaga H, Ueda M, Yanai N, Obinata M and Terasaki T (2000) mRNA expression and transport characterization of conditionally immortalized rat brain capillary endothelial cell lines; a new in vitro BBB model for drug targeting. *J Drug Target* **8**:357-370.
- Inui K, Masuda S and Saito H (2000) Cellular and molecular aspects of drug transport in the kidney. *Kidney Int* **58**:944-958.
- Kageyama T, Nakamura M, Matsuo A, Yamasaki Y, Takakura Y, Hashida M, Kanai Y, Naito

DMD# 22087

- M, Tsuruo T, Minato N and Shimohama S (2000) The 4F2hc/LAT1 complex transports L-DOPA across the blood-brain barrier. *Brain Res* **879**:115-121.
- Kido Y, Tamai I, Ohnari A, Sai Y, Kagami T, Nezu J, Nikaido H, Hashimoto N, Asano M and Tsuji A (2001) Functional relevance of carnitine transporter OCTN2 to brain distribution of L-carnitine and acetyl-L-carnitine across the blood-brain barrier. *J Neurochem* **79**:959-969.
- Koepsell H, Schmitt BM and Gorboulev V (2003) Organic cation transporters. *Rev Physiol Biochem Pharmacol* **150**:36-90.
- Kusuhara H, He Z, Nagata Y, Nozaki Y, Ito T, Masuda H, Meier PJ, Abe T and Sugiyama Y (2003) Expression and functional involvement of organic anion transporting polypeptide subtype 3 (Slc21a7) in rat choroid plexus. *Pharm Res* **20**:720-727.
- Kokubun H, Ouki M, Matoba M, Kubo H, Hoka S and Yago K (2005) Determination of oxycodone and hydrocotarnine in cancer patient serum by high-performance liquid chromatography with electrochemical detection. *Anal Sci* **21**:337-339.
- Mori S, Takanaga H, Ohtsuki S, Deguchi T, Kang YS, Hosoya K and Terasaki T (2003) Rat organic anion transporter 3 (rOAT3) is responsible for brain-to-blood efflux of homovanillic acid at the abluminal membrane of brain capillary endothelial cells. *J Cereb Blood Flow Metab* **23**:432-440.
- Mori S, Ohtsuki S, Takanaga H, Kikkawa T, Kang YS and Terasaki T (2004) Organic anion transporter 3 is involved in the brain-to-blood efflux transport of thiopurine nucleobase analogs. *J Neurochem* **90**:931-941.
- Nezu J, Tamai I, Oku A, Ohashi R, Yabuuchi H, Hashimoto N, Nikaido H, Sai Y, Koizumi A, Shoji Y, Takada G, Matsuishi T, Yoshino M, Kato H, Ohura T, Tsujimoto G, Hayakawa J, Shimane M and Tsuji A (1999) Primary systemic carnitine deficiency is caused by mutations in a gene encoding sodium ion-dependent carnitine transporter. *Nat Genet*

**21**:91-94.

- Ohta K, Inoue K, Hayashi Y and Yuasa H (2006) Molecular identification and functional characterization of rat multidrug and toxin extrusion type transporter 1 as an organic cation/H<sup>+</sup> antiporter in the kidney. *Drug Metab Dispos* **34**:1868-1874.
- Okura T, Ito R, Ishiguro N, Tamai I and Deguchi Y (2007) Blood-brain barrier transport of pramipexole, a dopamine D2 agonist. *Life Sci* **80**:1564-1571.
- Otuska M, Matsumoto T, Morimoto R, Arioka S, Omote H and Moriyama Y (2005) A human transporter protein that mediates the final excretion step for toxic organic cations. *Proc Natl Acad Sci* **50**:17923-17928.
- Ohtsuki S, Asaba H, Takanaga H, Deguchi T, Hosoya K, Otagiri M and Terasaki T (2002) Role of blood-brain barrier organic anion transporter 3 (OAT3) in the efflux of indoxyl sulfate, a uremic toxin: its involvement in neurotransmitter metabolite clearance from the brain. *J Neurochem* **83**:57-66.
- Pardridge WM (2005) The blood-brain barrier: bottleneck in brain drug development. *NeuroRx* **2**:3-14.
- Sipos H, Tőrocsik B, Tretter L and Adam-Vizi V (2005) Impaired regulation of pH homeostasis by oxidative stress in rat brain capillary endothelial cells. *Cell Mol Neurobiol* **25**:141-151.
- Takasato Y, Rapoport SI and Smith QR (1984) An in situ brain perfusion technique to study cerebrovascular transport in the rat. *Am J Physiol* **247**:H484-H493.
- Taylor CJ, Nicola PA, Wang S, Barrand MA and Hladky SB (2006) Transporters involved in regulation of intracellular pH in primary cultured rat brain endothelial cells. *J Physiol* **576**:769-785.
- Terada T, Masuda S, Asaka J, Tsuda M, Katsura T and Inui K (2006) Molecular cloning, functional characterization and tissue distribution of rat H<sup>+</sup>/organic cation antiporter



DMD# 22087

MATE1. *Pharm Res* **23**:1696-1701.

Terasaki T, Ohtsuki S, Hori S, Takanaga H, Nakashima E and Hosoya K (2003) New approaches to in vitro models of blood-brain barrier drug transport. *Drug Discov Today* **8**:944-954.

Tunblad K, Jonsson EN and Hammarlund-Udenaes M (2003) Morphine blood-brain barrier transport is influenced by probenecid co-administration. *Pharm Res* **20**:618-623.

Tsuji A (2005) Small molecular drug transfer across the blood-brain barrier via carrier-mediated transport systems. *NeuroRx* **2**:54-62.

Yamazaki M, Terasaki T, Yoshioka K, Nagata O, Kato H, Ito Y and Tsuji A (1994a) Carrier-mediated transport of H1-antagonist at the blood-brain barrier: mepyramine uptake into bovine brain capillary endothelial cells in primary monolayer cultures. *Pharm Res* **11**: 975-978.

Yamazaki M, Terasaki T, Yoshioka K, Nagata O, Kato H, Ito Y and Tsuji A (1994b) Carrier-mediated transport of H1-antagonist at the blood-brain barrier: a common transport system of H1-antagonists and lipophilic basic drugs. *Pharm Res* **11**:1516-1518.

Yamazaki M, Fukuoka H, Nagata O, Kato H, Ito Y, Terasaki T and Tsuji A (1994c) Transport mechanism of an H1-antagonist at the blood-brain barrier: transport mechanism of mepyramine using the carotid injection technique. *Biol Pharm Bull* **17**:676-679.

DMD# 22087

## Footnotes

This work was supported in part by a Grant-in-Aid for Scientific Research and a Grant-in-Aid for Young Scientists provided by The Ministry of Education, Culture, Sports, Science and Technology.

## Legends for figures

### **Fig. 1 Time course of uptake of oxycodone (A) and [<sup>3</sup>H]pyrilamine (B) into TR-BBB13 cells.**

Uptake of oxycodone (10  $\mu$ M) or [<sup>3</sup>H]pyrilamine (90 nM) was measured at 37°C (○) and 4°C (●). Each point represents the mean  $\pm$  S.E. of three or four determinations. Asterisks show a significant difference, \*P<0.05, \*\*P<0.01, \*\*\*P<0.001 vs 37°C.

### **Fig. 2 Concentration-dependence of uptake of oxycodone (A) and [<sup>3</sup>H]pyrilamine (B) into TR-BBB13 cells.**

Inset, Eadie-Hofstee plots. v, uptake in nmol/mg protein/15 sec. Substrate concentration in mM. Uptake of oxycodone or [<sup>3</sup>H]pyrilamine was measured at 37°C for 15 or 10 sec, respectively. Each point represents the mean  $\pm$  S.E. from three or four determinations.

### **Fig. 3 Trans-stimulation effects on oxycodone (A) and [<sup>3</sup>H]pyrilamine (B) uptake into TR-BBB13 cells.**

The cells were preincubated for 20 min in the absence (control) and presence of pyrilamine (250  $\mu$ M) or oxycodone (1 mM). Then, the uptake of oxycodone (30  $\mu$ M) or [<sup>3</sup>H]pyrilamine (90 nM) was measured at 37°C for 15 or 10 sec, respectively. Each column represents the mean  $\pm$  S.E. of three or four determinations. Asterisks show a significant difference, \*\*P<0.01 vs control.

### **Fig. 4 Lineweaver-Burk plot of mutual inhibitory effects on uptakes of oxycodone (A) and [<sup>3</sup>H]pyrilamine (B) into TR-BBB13 cells.**

Oxycodone uptake was measured at 37°C for 15 sec in the presence (●) or absence (○) of unlabeled pyrilamine (30  $\mu$ M). [<sup>3</sup>H]Pyrilamine uptake was also measured at 37°C for 10 sec

DMD# 22087

in the presence (●) or absence (○) of oxycodone (500  $\mu$ M). Each point represents the mean  $\pm$  S.E. of three or four determinations

**Fig. 5 Effect of ATP-depletion on uptakes of oxycodone (A) and [ $^3$ H]pyrilamine (B) into TR-BBB13 cells.**

Uptake of oxycodone (30  $\mu$ M) was measured at 37°C for 15 sec in the absence and presence of 25  $\mu$ M rotenone or 0.1 % sodium azide. Rotenone and sodium azide were preincubated for 20 min. Each column represents the mean  $\pm$  S.E. of three or four determinations. Asterisks show a significant difference, \*\*P<0.01 *vs* control.

**Fig. 6 Effects of sodium-replacement and membrane potential on uptakes of oxycodone (A, B) and [ $^3$ H]pyrilamine (C, D) into TR-BBB13 cells.**

Uptakes of oxycodone (30  $\mu$ M) and [ $^3$ H]pyrilamine (80 nM) were measured at 37°C for 15 and 10 sec, respectively, in sodium-containing (control) or sodium-free (replaced with N-methylglucamine) buffer. The mixtures were preincubated with valinomycin (10  $\mu$ M) for 10 min. Each column represents the mean  $\pm$  S.E. of three or four determinations.

**Fig. 7 Effects of extracellular pH and protonophore treatment on uptakes of oxycodone (A) and [ $^3$ H]pyrilamine (B), and effect of intracellular pH on uptakes of oxycodone (C) and [ $^3$ H]pyrilamine (D) into TR-BBB13 cells.**

Uptakes of oxycodone (30  $\mu$ M) and [ $^3$ H]pyrilamine (90 nM) were measured at 37°C for 15 and 10 sec, respectively, in the absence and presence of 10  $\mu$ M p-trifluoromethoxyphenyl-hydrazone (FCCP). The mixtures were preincubated with FCCP for 10 min. The cells were preincubated with incubation medium (pH 7.4) in the absence (Control and Acute) or presence (Pre) of 30 mM ammonium chloride for 20 min. Then, the

DMD# 22087

preincubation medium was removed, and the cells were incubated with 30  $\mu$ M oxycodone (pH 7.4 and pH 8.4) in the absence (Control and Pre) or presence (Acute) of 30 mM ammonium chloride for 15 sec at 37°C . Each column represents the mean  $\pm$  S.E. of three or four determinations.

**Fig. 8 Brain uptake of oxycodone in rats determined by the in situ brain perfusion method.**

(A) The perfusate containing oxycodone (30  $\mu$ M) with or without pyrilamine (1 mM) was perfused into the brain hemisphere through the carotid arterial catheter at a rate of 4.9 mL/min for 0-30 sec. (B) The brain perfusion of oxycodone was measured in perfusate of pH 7.4 or pH 8.4 in the absence and presence of 1 mM pyrilamine. The brain uptake was correlated with the rapidly equilibrating space of oxycodone. Each value represents the mean  $\pm$  S.E. of three or four determinations.

**Table 1 Inhibitory effects of selected compounds on uptake of oxycodone or [<sup>3</sup>H]pyrilamine by TR-BBB13 cells**

	Concentration (mM)	Relative uptake (% of control)	
		Oxycodone	[ <sup>3</sup> H]Pyrilamine
Control		100	100
Pyrilamine	1	11.1 ± 5.7**	6.78 ± 0.60**
Quinidine	1	9.26 ± 0.5**	3.37 ± 0.30**
Verapamil	1	9.54 ± 0.2**	3.95 ± 0.15**
Amantadine	1	20.1 ± 1.9**	10.6 ± 1.08**
Morphine	1	58.4 ± 6.6*	39.1 ± 1.8**
TEA	1	93.5 ± 5.9	95.2 ± 8.9
MPP	1	66.8 ± 11	89.9 ± 1.7
Serotonin	1	49.2 ± 6.8**	69.8 ± 6.5**
Choline	1	103 ± 9.6	79.3 ± 2.0*
Hemicholinium-3	0.15	71.8 ± 22.4	76.2 ± 2.7**
Corticosterone	1	96.7 ± 6.6	110 ± 4
Ergothioneine	1	86.3 ± 3.0	97.1 ± 8.2
L-Carnitine	1	93.9 ± 13	95.7 ± 7.1
p-Aminohippuric acid	1	83.6 ± 9.2	91.6 ± 4.1
Digoxin	0.1	102 ± 2.2	105 ± 6

Uptake of oxycodone (30 μM) was measured for 15 sec at 37°C in transport medium (pH 7.4) containing each compound. Each value represents mean ± S.E. of three or four determinations. Asterisks show a significant difference, \*P<0.05, \*\*P<0.01 vs control. TEA: tetraethylammonium, MPP: 1-methyl-4-phenylpyridinium.

**Table 2 mRNA expression levels of organic cation transporters in TR-BBB13 cells, and in brain and kidney of rats as determined by quantitative RT-PCR analysis.**

Target mRNA	Target mRNA (copies /ng total RNA)		
	TR-BBB13	Brain	Kidney
rOCT1	0.7 ± 0.4	N.D.	10313 ± 328
rOCT2	2.3 ± 0.1	39.6 ± 6.6	45160 ± 443
rOCT3	2.3 ± 0.6	381 ± 25	45.6 ± 0.8
rOCTN1	8.9 ± 0.3	531 ± 30	2517 ± 44
rOCTN2	1254 ± 92	564 ± 3	11527 ± 347
rMATE1	1.3 ± 0.6	15.7 ± 6.3	23519 ± 2335
rGAPDH	4124 ± 90	2722 ± 174	3386 ± 931

Each value represents the mean ± S.E. of three determinations. N.D.: not detected.

OCT, OCTN: organic cation transporter, MATE: multidrug and toxin extrusion, GAPDH : glyceraldehyde-3-phosphate dehydrogenase.

Fig. 1A

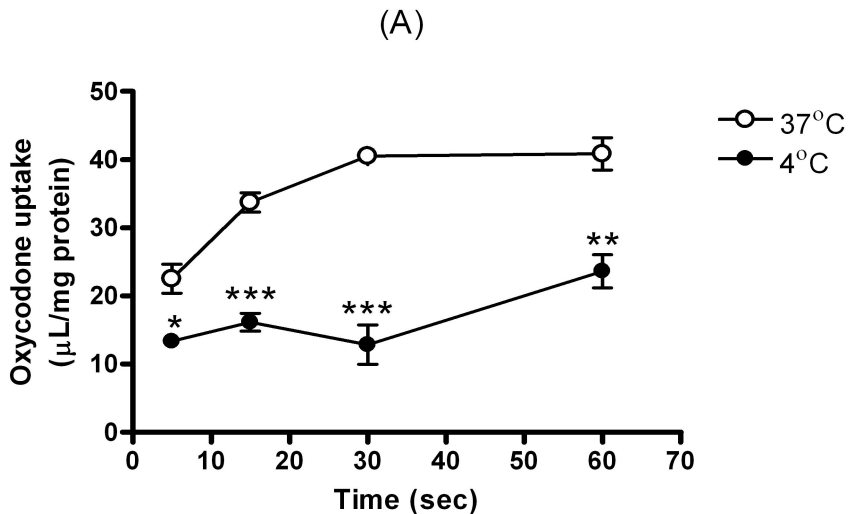
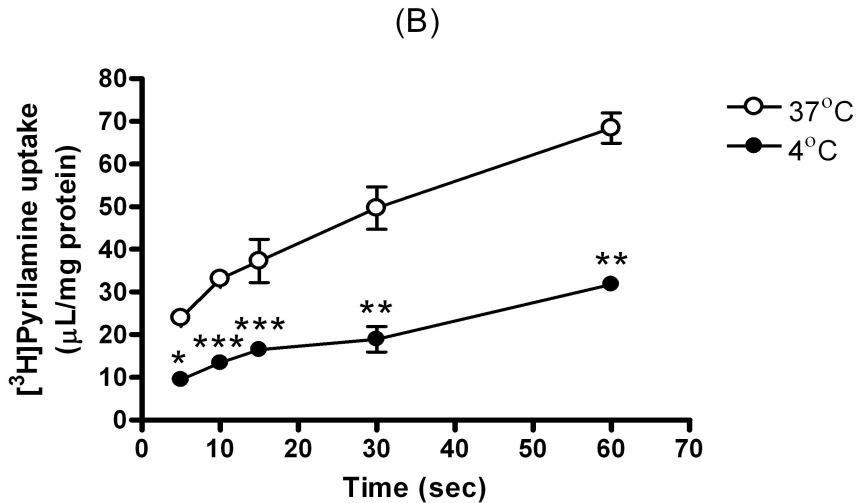




Fig. 1B



(A)

Fig. 2A

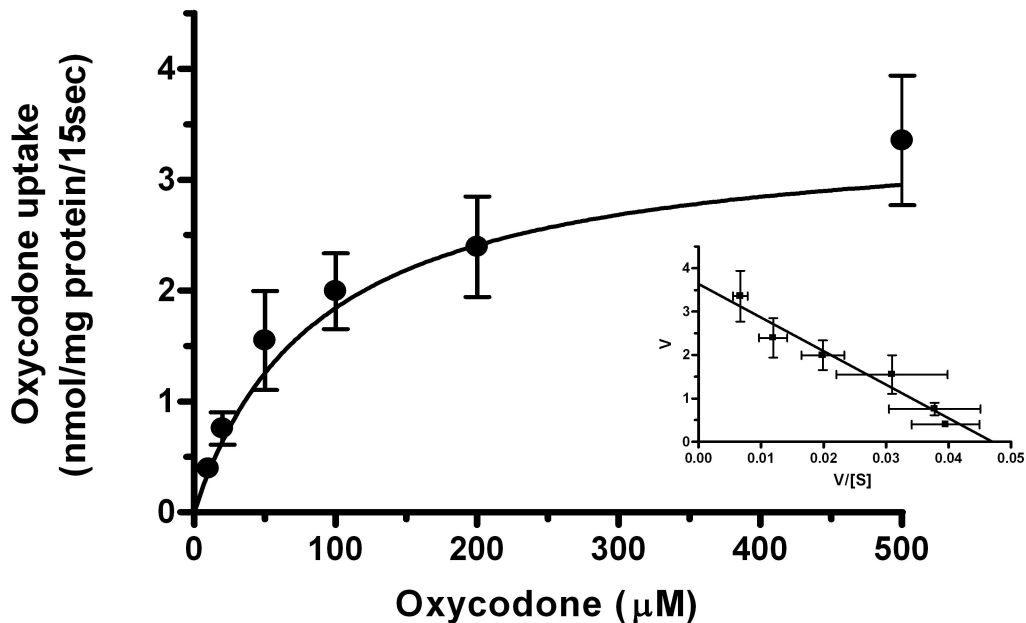


Fig. 2B

(B)

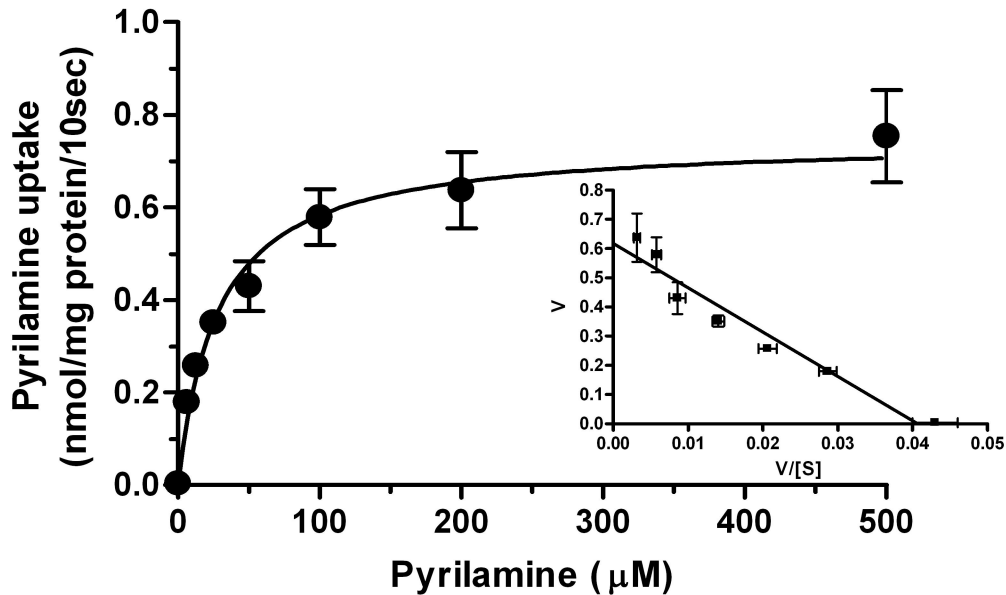


Fig. 3

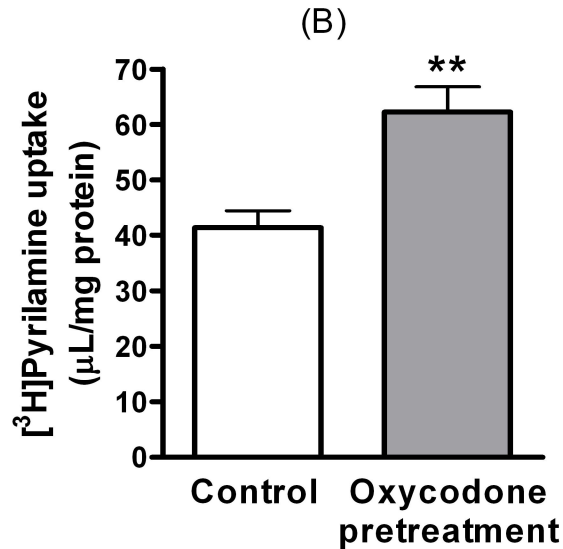
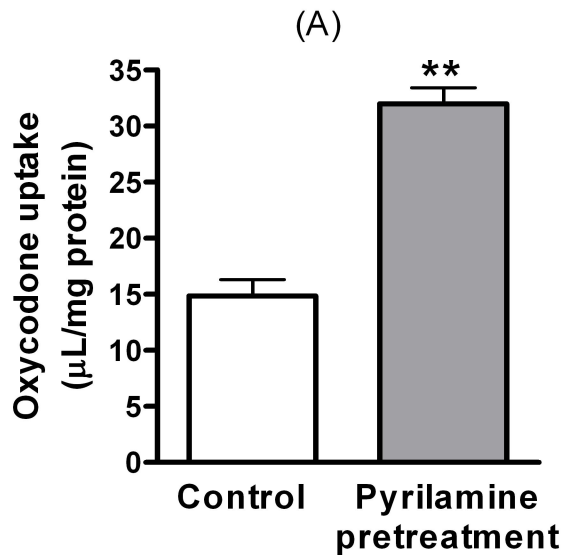


Fig. 4

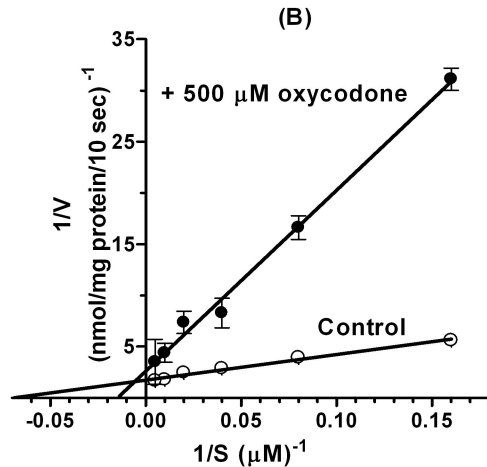
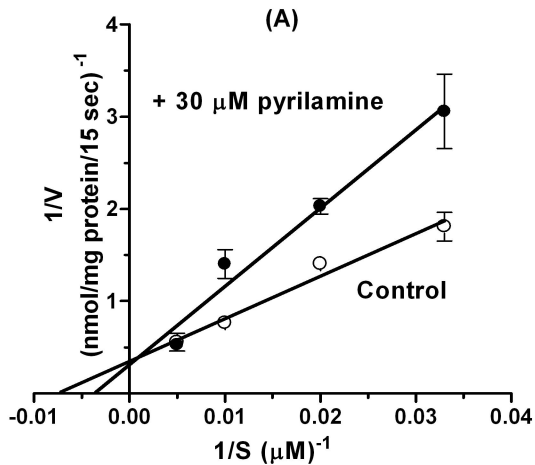


Fig. 5

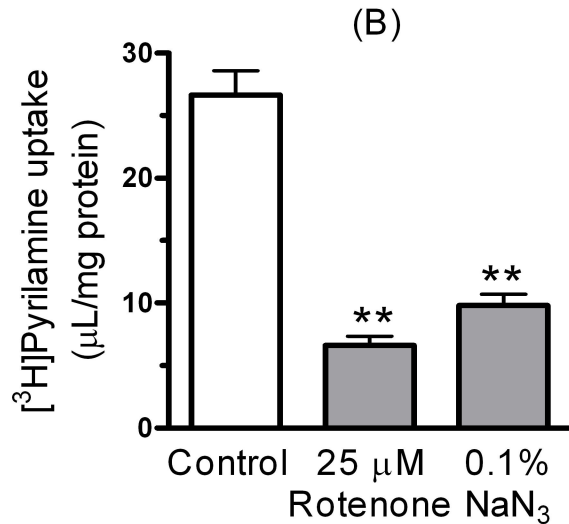
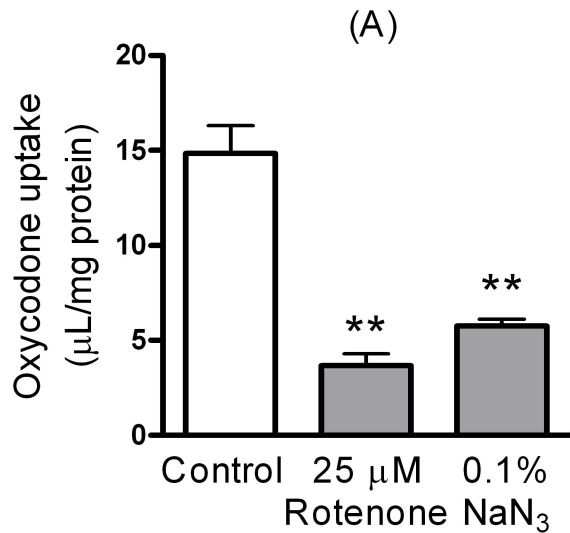
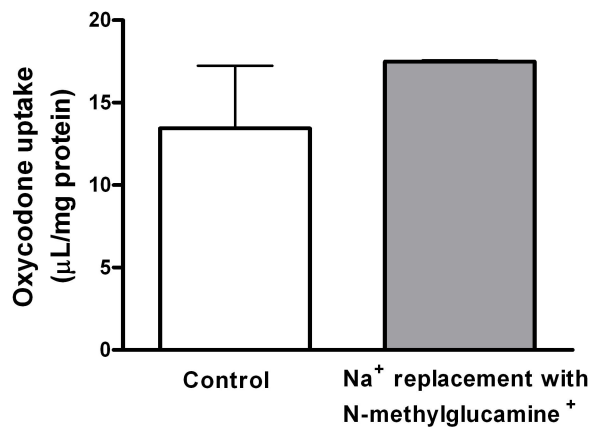
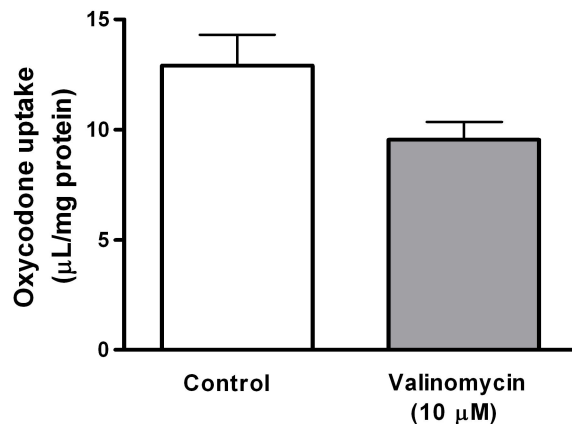


Fig. 6

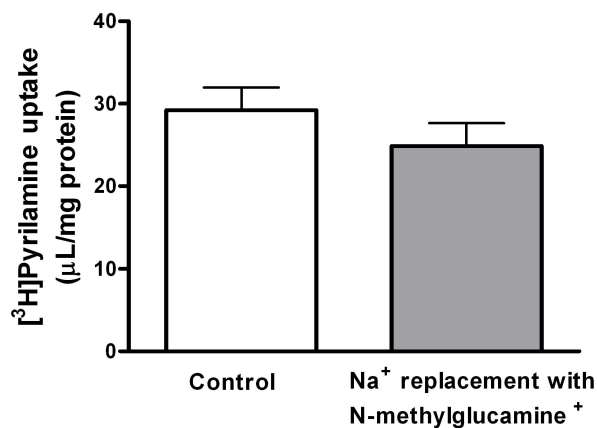
(A)



(B)



(C)



(D)

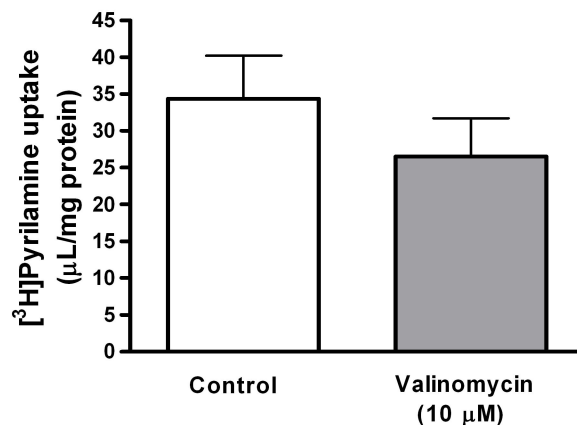


Fig. 7A,B

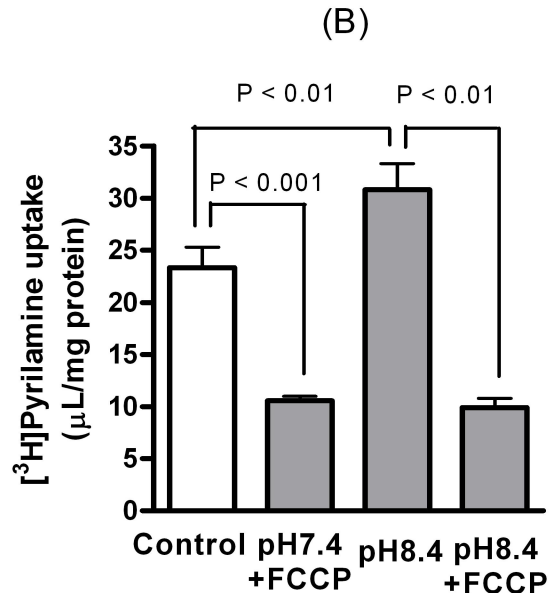
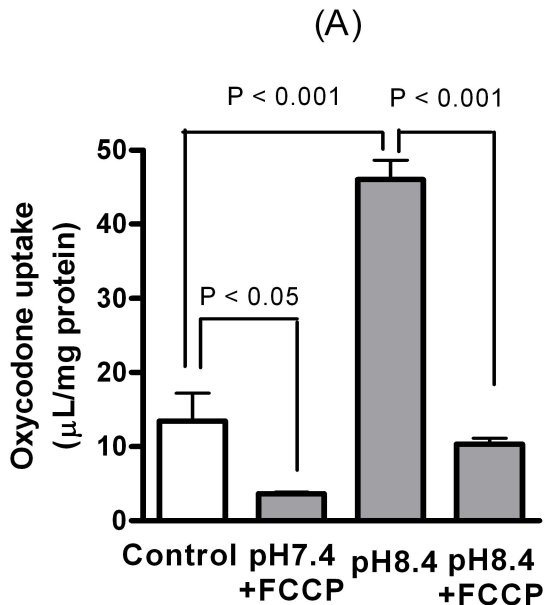
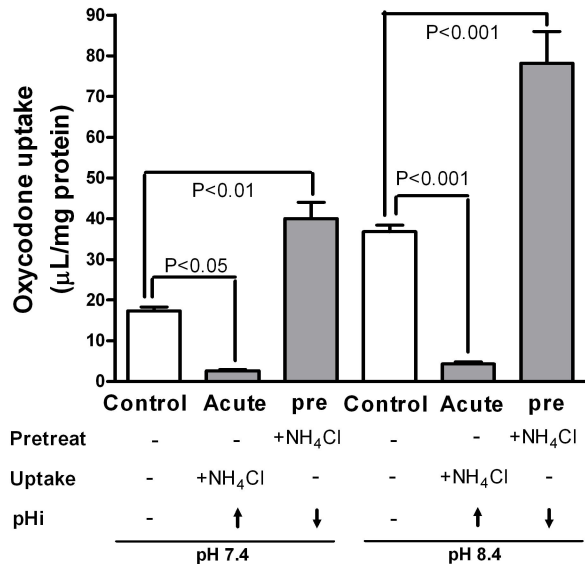




Fig. 7C,D

(C)



(D)

